

The spatial coherence of weakly interacting one-dimensional non-equilibrium Bosonic quantum fluids

Vladimir N. Gladilin,^{1,2} Kai Ji,¹ and Michiel Wouters¹

¹*TQC, Universiteit Antwerpen, Universiteitsplein 1, B-2610 Antwerpen, Belgium*

²*INPAC, KU Leuven, Celestijnenlaan 200D, B-3001 Leuven, Belgium*

(Dated: October 1, 2018)

We present a theoretical analysis of spatial correlations in a one-dimensional driven-dissipative non-equilibrium condensate. Starting from a stochastic generalized Gross-Pitaevskii equation, we derive a noisy Kuramoto-Sivashinsky equation for the phase dynamics. For sufficiently strong interactions, the coherence decays exponentially in close analogy to the equilibrium Bose gas. When interactions are small on a scale set by the nonequilibrium condition, we find through numerical simulations a crossover between a Gaussian and exponential decay with peculiar scaling of the coherence length on the fluid density and noise strength.

The spatial coherence is one of the key observables of quantum degenerate Bose gases. While for Bose gases in thermal equilibrium, its behavior is thoroughly understood [1], the case of non-equilibrium Bose gases has received much less attention. The non-equilibrium condition is typically of importance for photonic systems, where due to the limited reflectivity of any real mirrors, the photon life time is usually too short to achieve true thermal equilibrium. A steady state arises instead thanks to the balancing of external pumping and losses. Also in the non-equilibrium situation, the spatial coherence remains a central observable, that is experimentally accessible for photons [2]. Despite the existence of spatially extended lasers for many decades [3], the interest in the fundamental properties of nonequilibrium quantum fluids has come quite recently, with the advent of microcavity polariton quantum fluids [4]. Polaritons are the quasi-particles that arise from the strong coupling between a photon mode and an excitonic excitation in a quantum well. They inherit the good coherence properties from the photon together with substantial interactions from the exciton. Experimentally, spatial coherence measurements have been performed for two-dimensional polariton quantum fluids by many groups [2, 5–8].

In most experiments with microcavity polaritons, the nonequilibrium condition is essential to understand their properties. It gives for instance rise to a flow in the steady state [8–10], that can assume the form of quantized vortices [11] or feature more complicated patterns [12]. From the theoretical point of view, these nonequilibrium flows can be understood on a mean field level, from a generalized Gross-Pitaevskii equation (gGPE) [13, 14], that is of the same type as the complex Ginzburg-Landau equation. In this Letter, we will consider an equation in the form [4]

$$i\hbar\frac{\partial}{\partial t}\psi = \left[-\frac{\hbar^2\nabla^2}{2m} + g|\psi|^2 + \frac{i}{2} \left(\frac{P}{1+|\psi|^2/n_s} - \gamma \right) \right] \psi. \quad (1)$$

Here m is the effective mass and interactions are de-

scribed by a contact interaction with strength g . The imaginary term in the square brackets on the right hand side describes the saturable pumping (with strength P and saturation density n_s), that compensates for the losses (γ). The physical origin of the pumping term for exciton-polariton condensates is an excitonic reservoir that is excited by a nonresonant laser. For the case of ordinary lasing in the weak coupling regime, it describes emission of photons from the inverted electronic transition. In laser physics, a wide variety of spatial optical patterns, described by gGP-like equations, have been observed [3].

In homogeneous systems, a simple uniform steady state solution of Eq.(1) exists. When the pumping exceeds the losses ($P > \gamma$), it reads $\psi_0 = \sqrt{n_0}e^{-i\mu t/\hbar}$, where $n_0 = n_s(P/\gamma - 1)$ and the oscillation frequency is determined by the interaction energy $\mu = gn_0$. For the description of the spatial coherence, fluctuations have to be added to the gGPE. We will consider the simplest case of spatially uncorrelated and spectrally white noise. We thus supplement the right hand side of the gGPE with a stochastic term $\sqrt{D}dW/dt$, where the complex stochastic increments have the correlation function $\langle dW^*(x, t)dW(x', t') \rangle = 2\delta(x - x')\delta_{t, t'}dt$. The coefficient D describes the strength of the fluctuations. The contributions from quantum fluctuations can for example be derived within a truncated Wigner approximation, leading to $D \sim \gamma$ [15].

As usual for the calculation of the coherence of a low-dimensional system, we perform the Madelung transformation $\psi = \sqrt{n}e^{i\theta}$ to describe the complex field in terms of its density and phase. This is most convenient, because the long-range part of the spatial coherence is dominated by phase fluctuations. In the regime of weak noise, the density fluctuations are small and we can expand the interaction and gain saturation terms up to linear order in $\delta n = n - n_0$. Because the low-momentum density fluctuations relax much faster than the long wavelength phase fluctuations, they can be adiabatically eliminated to derive an equation of the phase dynamics only (see

supplemental information for a derivation and a numerical check of the equivalence with Eq. (1)). It reads in Ito form

$$d\tilde{\theta} = \left[\tilde{\mu} \nabla_{\tilde{x}}^2 \tilde{\theta} - \nabla_{\tilde{x}}^4 \tilde{\theta} - (\nabla_{\tilde{x}} \tilde{\theta})^2 \right] d\tilde{t} + d\tilde{W}. \quad (2)$$

Here, the increment $d\tilde{W}$ in Eq. (2) is a real stochastic variable with correlation function $\langle d\tilde{W}(\tilde{x}, \tilde{t}) d\tilde{W}(\tilde{x}', \tilde{t}') \rangle = \delta(\tilde{x} - \tilde{x}') \delta_{\tilde{t}, \tilde{t}'} dt$. We have furthermore introduced the dimensionless variables $\tilde{x} = x/l_*$, $\tilde{t} = t/t_*$ and rescaled the phase as $\tilde{\theta} = \theta/\theta_*$. The length scale reads

$$l_* = \left(\frac{\hbar^2}{2m} \right)^{4/7} \eta^{3/7} \left(\frac{D}{\hbar n_0} \right)^{-1/7}. \quad (3)$$

Note its very weak dependence on the physical parameters n_0 and D . The time and phase scales read,

$$t_* = \hbar \left(\frac{\hbar^2}{2m} \right)^{2/7} \eta^{5/7} \left(\frac{D}{\hbar n_0} \right)^{-4/7}, \quad (4)$$

$$\theta_* = \left(\frac{\hbar^2}{2m} \right)^{-1/7} \eta^{1/7} \left(\frac{D}{\hbar n_0} \right)^{2/7}. \quad (5)$$

They depend on the parameter η , that is a property of the gain medium and can be written as $\eta = (1 + n_s/n_0)\gamma^{-1}$, showing that it decreases in our saturable gain model (1) for increasing density n_0 . The interaction energy, rescaled as $\tilde{\mu} = \mu/\mu_*$ where

$$\mu_* = \frac{1}{2} \left(\frac{\hbar^2}{2m} \right)^{-1/7} \eta^{-6/7} \left(\frac{D}{\hbar n_0} \right)^{2/7}, \quad (6)$$

remains as the only control parameter in the equation. Note that in the absence of gain saturation $\eta \rightarrow \infty$ (obtained in the limit $\gamma \rightarrow 0$), the time scale t_* diverges. The physical reason is that gain saturation is the only damping mechanism in our model. We have verified that a small energy relaxation term [19] does not have a qualitative impact on the results presented below.

The phase equation (2) is of the form of the noisy Kuramoto-Sivashinsky equation (KSE) [16]. The KSE equation has a wide range applications, covering e.g. flame fronts [17] and reaction-diffusion systems [18], as well as transverse pattern formation in lasers [20, 21].

The noisy KSE (2) has been studied in the context of kinetic surface roughening [23]. It has been shown [22] that it belongs to the universality class of the celebrated Kardar-Parisi-Zhang (KPZ) equation [24] (Eq. (2) without the fourth order derivative; for a review, see [25]). To the best of our knowledge, the spatial correlations of the noisy KSE have however not been systematically analyzed as a function of the control parameter $\tilde{\mu}$.

Let us start with the case of repulsive interactions $\tilde{\mu} > 0$ (in equilibrium, this is the only meaningful case because attractive interactions lead to a collapse) and defer attractive interactions to the end. The linearized version

of Eq. (2) is then a good starting point to understand the momentum distribution. It reads

$$\langle |\tilde{\theta}_{\tilde{k}}|^2 \rangle = \frac{1}{2(\tilde{\mu}\tilde{k}^2 + \tilde{k}^4)}, \quad (7)$$

where $\tilde{k} = kl_*$ is the rescaled momentum. The denominator represents the square of the Bogoliubov excitation spectrum $\tilde{\omega}_B^2(k) = \tilde{\mu}\tilde{k}^2 + \tilde{k}^4$.

The quadratic term dominates for wave vectors $\tilde{k} < \sqrt{\tilde{\mu}}$. In this region, the phase dynamics reduces to the KPZ equation, that was used for polaritons by Altman *et al.* [26]. Its relevance in the context of equilibrium quantum fluids was also pointed out in recent works on the dynamical structure factor of 1D bosons, both in the weakly [27] and the strongly [28] interacting limits.

So far, the discussion is valid for arbitrary dimensionality, but now we will restrict to a one-dimensional system, where the nonlinear term in the KPZ equation leaves the solution of the linearized equation invariant. The momentum distribution of the phase field is then given by Eq. (7). This corresponds to the quadratically decaying momentum distribution at long wavelengths as in 1D finite temperature equilibrium condensates. Eq. (7) implies with the Fourier relation

$$\overline{\delta\theta^2}(x) = \frac{1}{L} \sum_k \langle |\theta_k|^2 \rangle [\cos(kx) - 1] \quad (8)$$

that the phase-phase correlator decreases for long distances linearly with the distance

$$\overline{\delta\theta^2}(x) \equiv \langle \tilde{\theta}(x)\tilde{\theta}(0) \rangle - \langle \tilde{\theta}^2(0) \rangle = -\tilde{x}/(4\tilde{\mu}), \quad (9)$$

For the evaluation of the characteristic function that determines the shape of the spatial coherence function $g^{(1)}(x) = \langle \psi^\dagger(x)\psi(0) \rangle$, the second cumulant approximation is exact thanks to the Gaussian nature of the phase field in the solution of the KPZ equation [25]. For the correlation length in the exponential decay $\exp\{i[\theta(x) - \theta(0)]\} = \exp[-\delta\theta^2(x)]$, we then recover the expression for the coherence length $\ell_c = 4\hbar^2 n \eta \mu / (Dm)$, that was derived in Ref. [29]. An appealing correspondence with the equilibrium case [$\ell_c^{\text{eq.}} = 2n\hbar^2 / (k_B T m)$] can be made by identifying the temperature T with the noise strength and the mass with the ‘effective mass’ $m\eta/\mu$, that quantifies the curvature of the imaginary part of the dispersion. A salient feature of this result is that the coherence length tends to zero in the absence of interactions. The linearized theory thus leads to the prediction that a repulsive nonlinearity is essential for the spatial coherence of a nonequilibrium condensate or a laser. The problem for vanishing interactions can be immediately seen from Eqs. (7) and (8), because the sum over momenta features an infrared divergence, due to the k^{-4} divergence of the momentum distribution.

In this case however, the nonlinear term in Eq. (2) does not keep the momentum distribution (7) obtained

in the linearized approximation invariant. We can expect on the basis of a previous analysis [22] of the noisy KSE that the nonlinear term actually keeps the system in the KPZ universality class, featuring a k^{-2} behavior of the momentum distribution. In order to investigate the spatial coherence for smaller interaction energy, we have performed numerical simulations.

Figure 1 present the momentum distribution of the phase field for various values of the interaction energy. Our numerics confirms the validity of the linearized approximation (7) for sufficiently strong repulsive interactions by the excellent agreement between the stars and the dash-dot-dot line for $\tilde{\mu} = 1.5$. This corresponds to the KPZ regime discussed above, where the nonlinearity of Eq. (2) does not affect the static correlation function. For the intermediate interaction strength on the other hand, pronounced differences between the linearized approximation (dash-dotted) and the numerical simulations (triangles) become apparent at low k .

For zero interaction strength, the discrepancy between the squares and the dashed line is dramatic: instead of the k^{-4} behavior predicted by the linearized approximation, the momentum distribution exhibits the same k^{-2} divergence as in the KPZ interacting regime. The prefactor in the low-momentum region turns out to be 1 within our numerical accuracy of a few percent. As can be seen from Fig. 1, for $\tilde{\mu} = 0$ the piecewise approximation to the momentum distribution

$$\langle |\tilde{\theta}_{\tilde{k}}|^2 \rangle = \begin{cases} \tilde{k}^{-2} & \text{for } \tilde{k} < 1/\sqrt{2} \\ \frac{1}{2}\tilde{k}^{-4} & \text{for } \tilde{k} > 1/\sqrt{2} \end{cases} \quad (10)$$

is excellent for almost all \tilde{k} , thanks to the sharp crossover between the \tilde{k}^{-4} and \tilde{k}^{-2} regions. This should be contrasted with the much smoother crossover – described by the analytic function (7) – for strong repulsive interactions (pink stars).

The scaled phase-phase correlator in real space is shown in Fig. 2. The large distance ($\tilde{x} \gg 1$) decay is dominated by the \tilde{k}^{-2} region in the Fourier expansion (8) and reads in the continuum limit $\delta\tilde{\theta}^2(\tilde{x}) = -\tilde{x}/2$. The short range phase fluctuations are obtained by expanding the cosine in Eq. (8) up to second order. It turns out that the low and high momentum regions contribute equally. The piecewise momentum distribution (10) leads to $\overline{\delta\tilde{\theta}^2}(\tilde{x}) = -\tilde{x}^2/\sqrt{2\pi^2}$, valid for $\tilde{x} \ll 1$. Within the second cumulant approximation, this leads to successive Gaussian and exponential decays for the first order spatial coherence function $g^{(1)}(x)$. The border between both regimes is determined by the length scale l_* .

In the exponential regime, we find for the correlation length $l_e = 2l_*\theta_*^{-2}$, featuring the peculiar scalings as a function of the physical quantities $l_e \propto n_0^{5/7}D^{-5/7}m^{-6/7}\eta^{1/7}$. Note the different scalings as a function of the physical parameters as compared to the

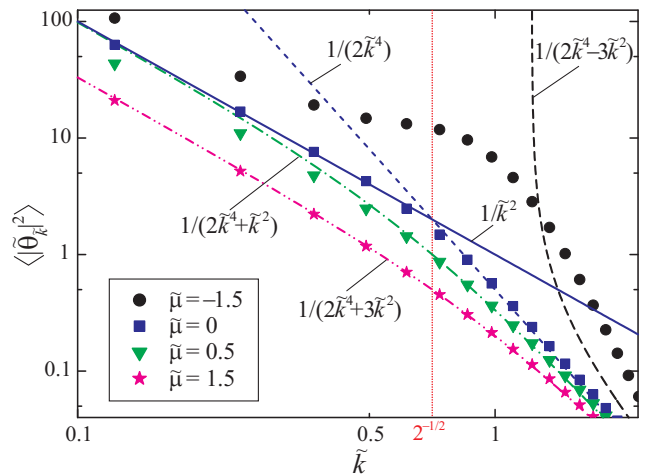


Figure 1. Numerically calculated momentum distribution of the phase field, $\langle |\tilde{\theta}_{\tilde{k}}|^2 \rangle$, as a function of \tilde{k} for $\tilde{\mu} = -1.5$ (circles), 0 (squares), 0.5 (triangles), and 1.5 (stars). The dashed, short-dash, dash-dot, and dash-dot-dot curves represent the momentum distribution given by Eq. (7) for $\tilde{\mu} = -1.5, 0, 0.5$, and 1.5, respectively. The function \tilde{k}^{-2} (solid line) approximates the calculated low-momentum behavior of $\langle |\tilde{\theta}_{\tilde{k}}|^2 \rangle$ in the absence of interactions. The dotted vertical line corresponds to the crossover between this behavior and a faster ($\propto \tilde{k}^{-4}$) decay at higher momenta.

regime of strong interactions. The Gaussian correlation length is $l_G = (2\pi^2)^{1/4}l_*\theta_*^{-1}\eta^{2/7}$ and scales as $l_G \propto n_0^{3/7}D^{-3/7}m^{-5/7}$. When the initial Gaussian decay is by many orders of magnitude, the long distance exponential tail becomes irrelevant. It is then meaningful to distinguish two regimes. The decay is dominantly Gaussian when the ‘phase scale’ θ_* is much larger than one, where it is dominantly exponential in the opposite limit. In terms of the physical parameters of the nonequilibrium Bose fluid, the decay is dominantly Gaussian for large noise and low density: $D > \hbar^2 n_0 / \sqrt{2\eta m}$.

Thanks to the sharp crossover of the momentum distribution between its two limiting behaviors, the piecewise approximation (10) actually leads to an accurate expression for the phase correlator at all distances. Its explicit form is given in the supplemental material. In Fig. 2, it is displayed with a dotted line, showing almost perfect agreement with the numerical results. Furthermore, the analytic formula allows us to do a straightforward extrapolation to infinite systems (open squares in Fig. 2). The good agreement between extrapolations starting from simulations with different sizes (not shown here) confirms good convergence of our results as a function of system size.

The above analysis was based on the assumption of the validity of the second cumulant approximation for the characteristic function $\langle \exp\{i[\theta(x) - \theta(0)]\} \rangle$. It is obviously applicable for small phase variations, when this correlator is well approximated by an expansion of the

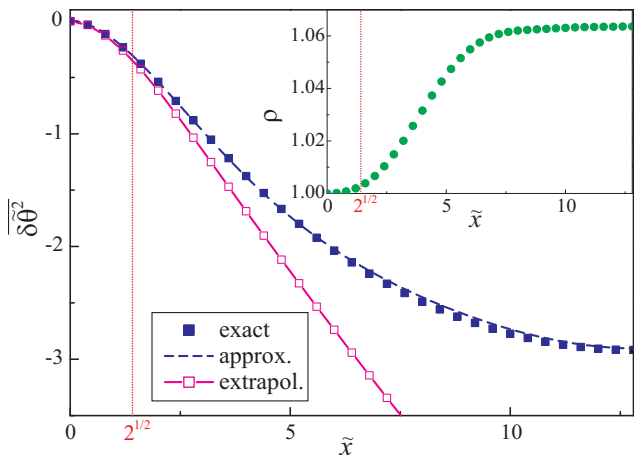


Figure 2. Phase-phase correlator in real space for $\tilde{\mu} = 0$, $L = 25.6l_*$ as given by the numerical simulations (full squares) and by the analytical formula resulting from the piecewise approximation (10) (dashed curve). The finite-size correction described by this formula has been used to extrapolate the numerical data to the case $L \rightarrow \infty$ (open squares). Inset: ratio $\rho(x) = \ln\langle \exp\{i[\theta(x) - \theta(0)]\} \rangle / \overline{\delta\theta^2}(x)$ calculated numerically for $\tilde{\mu} = 0$, $\theta_* = 1$, $L = 25.6l_*$.

exponentials up to the second order in θ . For Gaussian phase fluctuations, it is also guaranteed to hold, thanks to Wick's theorem. For the short wavelength fluctuations, the nonlinear term can be neglected, so that the phase increments are a linear combination of the input noise, and therefore guaranteed to be Gaussian by the central limit theorem. For the long wavelength components, that are crucially affected by the nonlinearity, this argument breaks down. In order to check the accuracy of the second cumulant approximation for the characteristic function, we have evaluated it numerically. In the inset to Fig. 2, we plot the ratio $\rho(x) = \ln\langle \exp\{i[\theta(x) - \theta(0)]\} \rangle / \overline{\delta\theta^2}(x)$ obtained for $\theta_* = 1$. Starting from $\rho = 1$ at $x \ll l_*$, this ratio slightly increases at $x \gtrsim \sqrt{2}l_*$ and apparently tends to saturate at even larger x . The shown behavior of $\rho(x)$ implies that the characteristic length for the exponential decay of the correlator $\langle \exp\{i[\theta(x) - \theta(0)]\} \rangle$ at long distances is about six percent smaller than the value l_e , which follows from the second cumulant approximation. It is worth mentioning that the statistical convergence of the calculation of the correlator $\langle \exp\{i[\theta(x) - \theta(0)]\} \rangle$ is much slower as compared to the calculation of the phase fluctuations $\overline{\delta\theta^2}$. Moreover, it is unfortunate that the correction to the second cumulant approximation depends on the parameter θ_* and hence on the strength of the noise, so that one cannot obtain the correlator $\langle \exp\{i[\theta(x) - \theta(0)]\} \rangle$ at different noise strengths by a simple rescaling. On the other hand, as seen from the inset to Fig. 2, even for the chosen value $\theta_* = 1$, which corresponds to a rather strong noise, the difference between the exact correlator and the second cumulant approximation remains moderate at all

distances.

Finally, we briefly discuss the case of attractive interactions. The equilibrium Bose gas is unstable with respect to the collapse of the gas because of the negative compressibility. The nonequilibrium counterpart is reflected in the linear instability of Eq. (2) for $\tilde{\mu} < 0$. In the nonequilibrium case however, the nonlinear term has a stabilizing effect, leading merely to a modulation of the phase (and correspondingly of the density) instead of a collapse. It is well known that for $\tilde{\mu} < 0$, the KSE without noise shows chaotic behavior, leading to effective stochastic dynamics at large scales, where the stochastic driving force stems from the linear instability [25]. The deterministic KSE with $\tilde{\mu} < 0$ and the stochastic KPZ equation belong to the same universality class [31]. Adding a stochastic term preserves this correspondence [22]. The dots in Fig. 1 show a momentum distribution for moderately attractive interactions ($\tilde{\mu} = -1.5$). The bump around $\tilde{k} = 1$ also appears in the absence of the noise [30] and corresponds in real space to a modulation of the phase. At small momenta, the momentum distribution shows the same k^{-2} behavior as in the case of repulsive or zero interactions, leading again to an exponential decay at the longest distance scales.

In conclusion, we have shown that the coherence of a nonequilibrium Bose gas is governed by the noisy Kuramoto-Sivashinsky equation and we have analyzed the effect of interactions. In contrast to linearized Bogoliubov theory, our study has shown that the coherence length does not vanish when interactions tend to zero, even though it is shorter than in the case of repulsive interactions. Moreover, in our numerical calculations, we have observed a deviation from Gaussian statistics. Our predictions could be verified experimentally in semiconductor microcavities, where the repulsive interaction strength can be varied by changing the exciton-photon detuning [32].

-
- [1] L. Pitaevskii and S. Stringari, *Bose-Einstein condensation*, Clarendon, Oxford (2003).
 - [2] J. Kasprzak *et al.*, Nature **443**, 409 (2006).
 - [3] K. Staliunas and V. J. Sánchez-Morcillo, *Transverse patterns in nonlinear optical resonators*, Springer, Heidelberg (2003).
 - [4] I. Carusotto and C. Ciuti, Rev. Mod. Phys. **85**, 299 (2013).
 - [5] R. Spano *et al.* New J. Phys. **14**, 075018 (2012).
 - [6] H. Deng, *et al.* Phys. Rev. Lett. **99**, 126403 (2007).
 - [7] E. A. Cerda-Mndez Phys. Rev. Lett. **105**, 116402 (2010).
 - [8] E. Wertz *et al.* Nat. Phys. **6**, 860 (2010).
 - [9] M. Richard, J. Kasprzak, R. Romestain, R. André, and L. S. Dang, Phys. Rev. Lett. **94**, 187401 (2005).
 - [10] M. Wouters, I. Carusotto and C. Ciuti, Phys. Rev. B **77**, 115340 (2008).
 - [11] K. Lagoudakis *et al.* Nat. Phys. **4**, 706 (2008).
 - [12] P. Cristofolini *et al.* Phys. Rev. Lett. **110**, 186403 (2013).

- [13] M. Wouters and I. Carusotto, Phys. Rev. Lett. **99**, 140402 (2007).
- [14] J. Keeling and N. Berloff, Phys. Rev. Lett. **100**, 250401 (2008).
- [15] M. Wouters and V. Savona, Phys. Rev. B **79**, 165302 (2009).
- [16] R. Cuerno and K. B. Lauritsen, Phys. Rev. E **52**, 4853 (1995).
- [17] G. Sivashinsky, Acta Astron., **4**, 1177 (1977).
- [18] Y. Kuramoto and T. Tsuzuki, Progr. Theoret. Phys. , **55**, 356 (1976).
- [19] L. P. Pitaevskii, Zh. Eksp. Teor. Fiz. **35**, **408** (1958) [Sov. Phys. JETP **35**, 282 (1959)].
- [20] R. Lefever, L. A. Lugiato, W. Kaige, N. B. Abraham and P. Mandel, Phys. Lett. A **135**, 254 (1989).
- [21] G. Huyet, M. C. Martinoni, J. R. Tredicce and S. Rica, Phys. Rev. Lett. **22**, 4027 (1995).
- [22] K. Ueno, H. Sakaguchi and M. Okamura, Phys. Rev. E **71**, 046138 (2005).
- [23] R. Cuerno, H. A. Makse, S. Tomassone, S. T. Harrington and H. E. Stanley, Phys. Rev. Lett. **75**, 4464 (1995).
- [24] M. Kardar, G. Parisi and Y.-C. Zhang, Phys. Rev. Lett. **56**, 889 (1986).
- [25] T. HalpinHealy, Y.-C. Zhang, Phys. Rept. , **254**, 215 (1995).
- [26] E. Altman, J. Toner, L. M. Sieberer, S. Diehl and L. Chen arxiv:11311.0876.
- [27] M. Kulkarni and A. Lamacraft, Phys. Rev. A **88**, 021603(R) (2013).
- [28] M. Arzamasovs, F. Bovo and D. M. Gangardt, arXiv:1309.2647.
- [29] A. Chiochetta and I. Carusotto, Eur. Phys. Lett. **102**, 67007 (2013).
- [30] K. Sneppen, J. Krug, M. Jensen, C. Jayaprakash, T. Bohr, Phys. Rev. A, **46**, 7531(R) (1992).
- [31] V.S. L'vov, V.V. Lebedev, M. Paton, I. Procaccia, Non-linearity **6**, 25 (1993).
- [32] M. Vladimirova *et al.*, Phys. Rev. B **82**, 075301 (2010); N. Takemura, S. Trebaol, M. Wouters, M. T. Portella-Oberli, B. Deveaud, arXiv:1310.6506.

SUPPLEMENTAL MATERIAL

Derivation of the phase equation

Inserting $\psi = \sqrt{n_0 + \delta n} e^{i\theta - i\mu t/\hbar}$ with $|\delta n| \ll n_0$ into Eq. (1), supplemented with a stochastic term $\sqrt{D}dW/dt$, and neglecting terms of the order of $(\delta n/n_0)^N$ with $N \geq 2$, one obtains

$$\frac{\hbar}{2} \frac{\partial}{\partial t} \frac{\delta n}{n_0} = -\frac{\hbar^2}{2m} \left[\nabla \frac{\delta n}{n_0} \nabla \theta + \left(1 + \frac{\delta n}{n_0} \right) \nabla^2 \theta \right] - \frac{1}{2\eta} \frac{\delta n}{n_0} + \sqrt{\frac{D}{n_0}} \frac{dW_n}{dt}, \quad (\text{S.1})$$

$$\hbar \frac{\partial}{\partial t} \theta = \frac{\hbar^2}{2m} \left[\frac{1}{2} \nabla^2 \frac{\delta n}{n_0} - (\nabla \theta)^2 \right] - \mu \frac{\delta n}{n_0} + \sqrt{\frac{D}{n_0}} \frac{dW_\theta}{dt}, \quad (\text{S.2})$$

where the real stochastic variables dW_n and dW_θ have correlators $\langle dW_n(x, t) dW_n(x', t') \rangle = \langle dW_\theta(x, t) dW_\theta(x', t') \rangle = \delta(x - x') \delta_{t, t'} dt$. Assuming that the characteristic time $\hbar\eta$, which determines relaxation of density fluctuations, is sufficiently short, the quantity $\delta n/n_0$ can be estimated from Eq. (S.1) as

$$\frac{\delta n}{n_0} \approx -\frac{\hbar^2 \eta}{m} \nabla^2 \theta + 2\eta \sqrt{\frac{D}{n_0}} \frac{dW_n}{dt}. \quad (\text{S.3})$$

When inserting $\delta n/n_0$ given by Eq. (S.3) into Eq. (S.2), we take into account that at small η -values under consideration (i) the inequality $\eta|\mu| \ll 1$ is satisfied for a moderate interaction strength and (ii) the contribution $\hbar^2 \eta (2m)^{-1} \sqrt{D/n_0} \nabla^2 (dW_n/dt)$ to the noise term can be neglected (except for the shortest length scale, which we are not interested in). Then one obtains for the phase equation the expression

$$\hbar \frac{\partial}{\partial t} \theta = \frac{\hbar^2}{2m} \left[-\frac{\hbar^2 \eta}{2m} \nabla^4 \theta - (\nabla \theta)^2 + 2\eta \mu \nabla^2 \theta \right] + \sqrt{\frac{D}{n_0}} \frac{dW_\theta}{dt}, \quad (\text{S.4})$$

which immediately transforms into Eq. (2) after substitutions $x = l_* \tilde{x}$, $t = t_* \tilde{t}$, $\theta = \theta_* \tilde{\theta}$, and $\mu_* \mu = \tilde{\mu}$ with l_* , t_* , θ_* and μ_* given by Eqs. (3) to (6). In the case of strong interactions, when the inequality $\eta|\mu| \ll 1$ is violated, one should simply replace the noise strength D in Eq. (S.4) [as well as in Eqs. (3) to (6)] with $D(1 + 2\eta\mu)^2$.

Fitting formula for the phase-phase correlator

We use the piecewise approximation of Eq. (10) for the momentum distribution $\langle |\hat{\theta}_{\mathbf{k}}|^2 \rangle$ in the absence of interactions. Then for a finite system of (dimensionless) size

\tilde{L} the scaled phase-phase correlator in real space can be represented as

$$\begin{aligned} \overline{\delta\theta^2}(\tilde{x}) \approx & \frac{\tilde{L}}{2\pi^2} \left[\sum_{\kappa=1}^{\infty} \frac{\cos(2\pi\kappa\tilde{x}/\tilde{L}) - 1}{\kappa^2} \right. \\ & \left. - \sum_{\kappa=\tilde{L}/(2\sqrt{2}\pi)}^{\infty} \frac{\cos(2\pi\kappa\tilde{x}/\tilde{L}) - 1}{\kappa^2} \right] \\ & + \frac{\tilde{L}^3}{(2\pi)^4} \sum_{\kappa=\tilde{L}/(2\sqrt{2}\pi)}^{\infty} \frac{\cos(2\pi\kappa\tilde{x}/\tilde{L}) - 1}{\kappa^4}. \end{aligned} \quad (\text{S.5})$$

Assuming that the system size is sufficiently large, $\tilde{L}/(2\sqrt{2}\pi) \gg 1$, the last two sums in Eq. (S.5) can be approximated by the corresponding integrals:

$$\begin{aligned} \overline{\delta\theta^2}(\tilde{x}) \approx & \frac{\tilde{L}}{2\pi^2} \sum_{\kappa=1}^{\infty} \frac{\cos(2\pi\kappa\tilde{x}/\tilde{L}) - 1}{\kappa^2} \\ & - \frac{\tilde{x}}{\pi} \int_{\tilde{x}/\sqrt{2}}^{\infty} dy \frac{\cos(y) - 1}{y^2} \\ & + \frac{\tilde{x}^3}{2\pi} \int_{\tilde{x}/\sqrt{2}}^{\infty} dy \frac{\cos(y) - 1}{y^4}. \end{aligned} \quad (\text{S.6})$$

These integrals as well as the infinite series in Eq. (S.6) can be easily evaluated [1] giving finally

$$\begin{aligned} \overline{\delta\theta^2}(\tilde{x}) = & -\frac{\tilde{x}}{2} \left[1 + \frac{2}{\pi} \text{si} \left(\frac{\tilde{x}}{\sqrt{2}} \right) \left(1 + \frac{\tilde{x}^2}{12} \right) \right] \\ & - \frac{2\sqrt{2}}{3\pi} \left[1 - \cos \left(\frac{\tilde{x}}{\sqrt{2}} \right) \left(1 + \frac{\tilde{x}^2}{8} \right) \right] \\ & + \frac{\tilde{x}}{4\sqrt{2}} \sin \left(\frac{\tilde{x}}{\sqrt{2}} \right) + \frac{\tilde{x}^2}{2\tilde{L}}, \end{aligned} \quad (\text{S.7})$$

where $\text{si}(x)$ is the sine integral [2]. The last term in Eq. (S.7) accounts for the finite size of the system.

Impact of phase correlations on the field-field correlator

In Fig. 3 we compare the functions $\exp[\overline{\delta\theta^2}(x)]$, obtained by rescaling the phase correlator $\overline{\delta\theta^2}(\tilde{x})$ (see the paper), to the first order spatial coherence function $g^{(1)}(x)/n_0$, calculated directly from Eq. (1), for the case of $g = 0$, $n_0 = n_s$ and three different values of the noise strength D . As follows from Fig. 3, while at weak noise (up to $D/D_0 \sim 10^{-3}$) the behavior of the field-field correlator $g^{(1)}(x)$ is perfectly described by the phase factor $\exp[\overline{\delta\theta^2}(x)]$, at higher noise strength an additional suppression of $g^{(1)}(x)/n_0$ by density fluctuations becomes non-negligible. Nevertheless, even in the case of $D/D_0 = 10^{-2}$ where the magnitude of density fluctuations is comparable to n_0 , the decay of $g^{(1)}(x)/n_0$ at

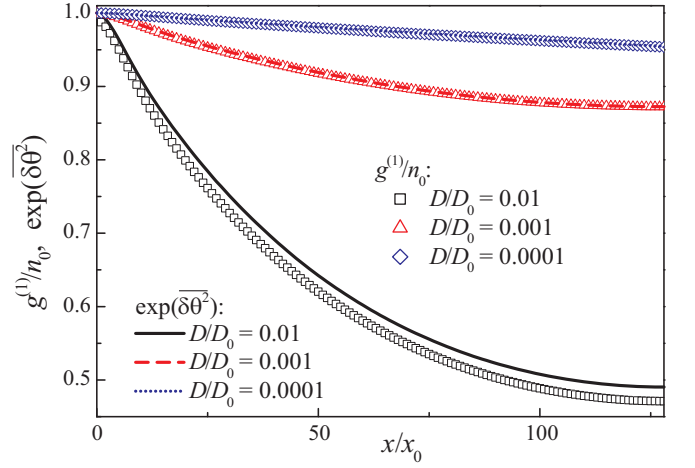


Figure 3. First order spatial coherence function $g^{(1)}(x)$ calculated numerically from Eq. (1) (open symbols) and the function $\exp[\overline{\delta\theta^2}(x)]$ (lines) for three different values of the noise strength D . The system size is $L = 1024x_0$ in the case of $D/D_0 = 0.0001$ and $L = 256x_0$ for the other two values of D/D_0 . Here $x_0 = \sqrt{\hbar n_s/(m\gamma n_0)}$, $D_0 = \hbar^3 n_0/(4m x_0)$.

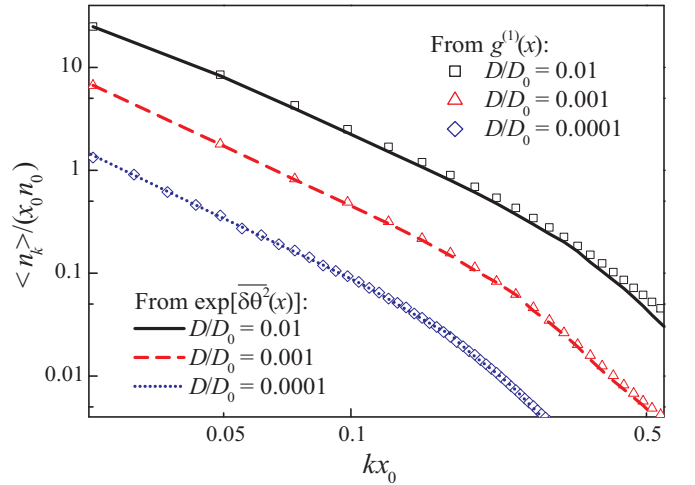


Figure 4. Momentum distribution functions calculated from the field-field correlator $g^{(1)}(x)$ (open symbols) and from the functions $\exp[\overline{\delta\theta^2}(x)]$ (lines) for three different values of the noise strength D . The system size is $L = 1024x_0$ in the case of $D/D_0 = 0.0001$ and $L = 256x_0$ for the other two values of D/D_0 . Here $x_0 = \sqrt{\hbar n_s/(m\gamma n_0)}$, $D_0 = \hbar^3 n_0/(4m x_0)$.

large distances is seen to be dominated by the effect of phase fluctuations.

In Fig. 4 we plot the momentum distribution functions, which correspond to $g^{(1)}(x)$ (open symbols) and $\exp[\overline{\delta\theta^2}(x)]$ (lines). In line with the discussion above, the long-wavelength behavior of the momentum distribution obtained by solving the “full” field equation (1) is completely determined by phase fluctuations. The effect of (short-range) density fluctuations is manifested only for relatively large momenta at sufficiently high noise

strength.

York: Gordon and Breach Science Publishers, 1986).

- [2] M. Abramowitz and I. A. Stegun, *Handbook of Mathematical Functions with Formulas, Graphs, and Mathematical Tables* (New York: Dover, 1972).

-
- [1] A. P. Prudnikov, Yu. A. Brychkov, and O. I. Marichev, *Integrals and series*, Vol.1: Elementary Functions (New